Journal of Computational Physics 227 (2008) 8769–8775

Contents lists available at ScienceDirect

Journal of Computational Physics

journal homepage: www.elsevier.com/locate/jcp

Short Note

On 1D diffusion problems with a gradient-dependent diffusion coefficient

S.C. Jardin [a,*], G. Bateman [b], G.W. Hammett [a], L.P. Ku [a]

[a] Princeton University, Plasma Physics Laboratory, P.O. Box 451, Princeton, NJ 08543, United States
[b] Lehigh University, Physics Department, 16 Memorial Drive East, Bethlehem, PA 18015, United States

ARTICLE INFO

Article history:
Received 20 March 2007
Received in revised form 7 April 2008
Accepted 28 June 2008
Available online 16 July 2008

Keywords:
Numerical methods
Newtons method
Diffusion equations
Magnetic fusion

In solving the 1D (flux surface averaged) transport equations for the temperatures, magnetic fields, and densities in the "evolving equilibrium" description of a tokamak [1], one increasingly encounters highly nonlinear thermal conductivity and diffusivity functions, such as GLF23 [2], that have a strong and non-analytic dependence on the temperature gradients. These arise from a subsidiary microstability based calculation in which the growth rates and hence transport coefficients are sensitive functions of these gradients [3]. When these nonlinear functions are interfaced with an existing transport framework that uses a standard implicit time advancement algorithm such as Crank-Nicolson or backward Euler [4], large non-physical oscillations can develop and, as a result, non-convergent solutions can occur. Here we describe a relatively simple modification to these implicit algorithms that cures this difficulty.

To illustrate the method, we start with a simple diffusion equation in cylindrical polar coordinates:

$$\frac{\partial T}{\partial t} = \frac{1}{r}\frac{\partial}{\partial r}\left[r\chi(T')\frac{\partial T}{\partial r}\right] + S. \tag{1a}$$

Now, define a new independent variable, Φ, proportional to the area (or the toroidal magnetic flux if a uniform longitudinal magnetic field is present), that is defined as: $\Phi \equiv r^2/4$. With this substitution, Eq. (1a) becomes

$$\frac{\partial T}{\partial t} = \frac{\partial}{\partial \Phi}\left[\Phi\chi(T')\frac{\partial T}{\partial \Phi}\right] + S. \tag{1b}$$

Here we have denoted the dependence of the thermal conductivity on $\partial T/\partial\Phi$ by $\chi(T')$. We normalize the domain to $0 \leqslant \Phi \leqslant 1$. Note that this has a steady-state solution for $\chi = 1$, $S = 1$, $T = 1 - \Phi$.

We apply a boundary condition of $T = 0$ at $\Phi = 1$, keep $S = 1$, and use the above solution as an initial condition. Now, define a function that mimics the critical gradient thermal diffusivity model GLF23:

* Corresponding author. Tel.: +1 609 243 2635; fax: +1 609 243 2662.
E-mail address: jardin@pppl.gov (S.C. Jardin).

0021-9991/$ - see front matter
doi:10.1016/j.jcp.2008.06.032

$$\chi(T') = \left\{ \begin{array}{ll} k(|T'| - T'_c)^{\alpha} + \chi_0 & \text{for } |T'| > T'_c \\ \chi_0 & \text{for } |T'| \leqslant T'_c \end{array} \right\}. \tag{2}$$

For definiteness, let $\chi_0 = 1.0$, $\alpha = 0.5$, $k = 10$, and $T'_c = 0.5$.

In order to finite difference Eq. (1b), we define a mesh going from 0 to 1. We make T_j a cell centered quantity, in which j goes from 1 to $N+1$. If we define the flux increment as $\Delta\Phi = 1/(N+1/2)$, then the temperature T_j is centered at location $\Phi_j = (j - \frac{1}{2})\Delta\Phi$. Thus, the temperature at $j = 1$ corresponds to a cell center located at $\Phi_1 = \frac{1}{2}\Delta\Phi$ and the boundary condition is applied as $T_{N+1} = 0$. There is no need for a ghost zone or boundary condition at $j = 0$. We first try solving this with a θ-implicit method (Crank-Nicolson corresponds to $\theta = 0.5$ and backward Euler to $\theta = 1.0$) with $s \equiv \Delta t/\Delta\Phi^2$:

$$\begin{aligned} T_j^{n+1} = T_j^n &+ s\theta\left\{\left[\Phi_{j+1/2}\chi\left(T'^n_{j+1/2}\right)\left(T^{n+1}_{j+1} - T^{n+1}_j\right)\right] - \left[\Phi_{j-1/2}\chi\left(T'^n_{j-1/2}\right)\left(T^{n+1}_j - T^{n+1}_{j-1}\right)\right]\right\} \\ &+ s(1-\theta)\left\{\left[\Phi_{j+1/2}\chi\left(T'^n_{j+1/2}\right)\left(T^n_{j+1} - T^n_j\right)\right] - \left[\Phi_{j-1/2}\chi\left(T'^n_{j-1/2}\right)\left(T^n_j - T^n_{j-1}\right)\right]\right\} + \Delta t S \end{aligned} \tag{3}$$

or, in tridiagonal form,

$$\begin{aligned} &A_j T^{n+1}_{j+1} - B_j T^{n+1}_j + C_j T^{n+1}_{j-1} + D_j = 0 \\ &A_j = s\theta\Phi_{j+1/2}\chi\left(T'^n_{j+1/2}\right) \\ &C_j = s\theta\Phi_{j-1/2}\chi\left(T'^n_{j-1/2}\right) \\ &B_j = 1 + A_j + C_j \\ &D_j = T^n_j + s(1-\theta)\left\{\Phi_{j+1/2}\chi\left(T'^n_{j+1/2}\right)\left(T^n_{j+1} - T^n_j\right) - \Phi_{j-1/2}\chi\left(T'^n_{j-1/2}\right)\left(T^n_j - T^n_{j-1}\right)\right\} + \Delta t S. \end{aligned} \tag{4}$$

The illustrations in Figs. 1 and 2 are the result of solving this with $n = 100$ zones, with a time step $\Delta t = 0.01$ (and 0.10), implicit parameter $\theta = 1.0$ for 200 (and 20) time steps. We plot the time history of the function and derivative at locations 10 and 90.

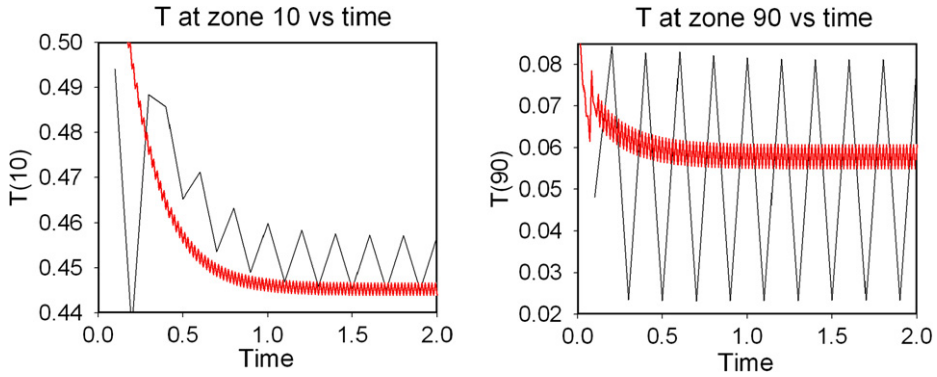

Fig. 1. Initial solution of Eq. (1) using backward Euler method corresponding to (3) with $\theta = 1$. Left plot is temperature vs. time at zone 10 and right is temperature vs. time at zone 90. Finely oscillating curves (red online) have $\Delta t = 0.01$, coarse oscillating curves have $\Delta t = 0.10$. (For interpretation of the references in colour in this figure legend, the reader is referred to the web version of this article.)

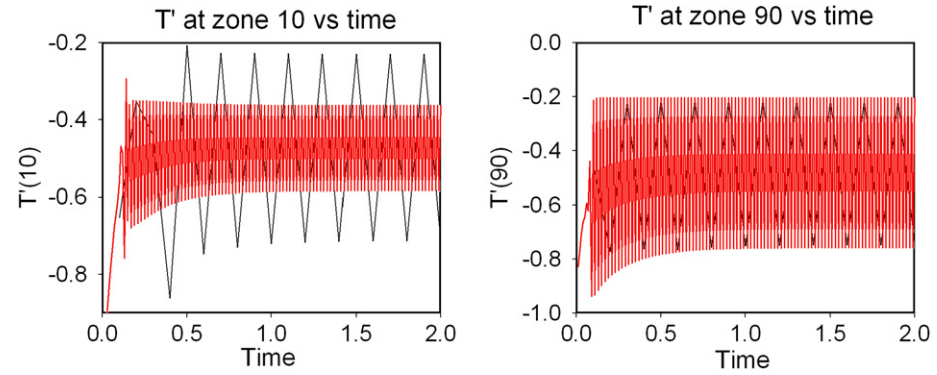

Fig. 2. Initial solution of Eq. (1) using backward Euler method (3). Left plot is $dT/d\Phi$ at zone 10 vs. time and right plot is at zone 90. Curves correspond to those in Fig. 1.

This is seen to be very noisy, with a large amplitude oscillation and is not obviously convergent. In order to improve the solution, we investigate a nonlinearly implicit method that would seek to evaluate the χ functions multiplying the advanced time derivatives also at the advanced times, i.e.:

$$T_j^{n+1} = T_j^n + s\theta\left\{\left[\Phi_{j+1/2}\chi\left(T'^n_{j+1/2}\right)\left(T_{j+1}^{n+1} - T_j^{n+1}\right)\right] - \left[\Phi_{j-1/2}\chi\left(T'^n_{j-1/2}\right)\left(T_j^{n+1} - T_{j-1}^{n+1}\right)\right]\right\} + s(1-\theta)\left\{\left[\Phi_{j+1/2}\chi\left(T'^n_{j+1/2}\right)\left(T_{j+1}^{n} - T_j^{n}\right)\right] - \left[\Phi_{j-1/2}\chi\left(T'^n_{j-1/2}\right)\left(T_j^{n} - T_{j-1}^{n}\right)\right]\right\} + \Delta t S. \tag{5}$$

We can derive a Newton's iteration to solve this by defining the modified coefficients corresponding to Newton iteration i (out of N):

$$A_j T_{j+1}^{n+i/N} - B_j T_j^{n+i/N} + C_j T_{j-1}^{n+i/N} + D_j = 0, \tag{6}$$

$$\begin{aligned}
A_j &= s\theta\Phi_{j+1/2}\left[\chi\left(T'^{n+(i-1)/N}_{j+1/2}\right) + \frac{\partial\chi}{\partial T'}T'^{n+(i-1)/N}_{j+1/2}\right]\\
C_j &= s\theta\Phi_{j-1/2}\left[\chi\left(T'^{n+(i-1)/N}_{j-1/2}\right) + \frac{\partial\chi}{\partial T'}T'^{n+(i-1)/N}_{j-1/2}\right]\\
B_j &= 1 + A_j + C_j\\
D_j &= T_j^n + s(1-\theta)\left[\Phi_{j+1/2}\chi\left(T'^n_{j+1/2}\right)\left(T_{j+1}^n - T_j^n\right) - \Phi_{j-1/2}\chi\left(T'^n_{j-1/2}\right)\left(T_j^n - T_{j-1}^n\right)\right]\\
&\quad + \Delta t S + s\theta\left[\begin{array}{l}\Phi_{j+1/2}\frac{\partial\chi}{\partial T'}T'^{n+(i-1)/N}_{j+1/2}\left(T_j^{n+(i-1)}/N - T_{j+1}^{n+(i-1)/N}\right)\\ +\Phi_{j-1/2}\frac{\partial\chi}{\partial T'}T'^{n+(i-1)/N}_{j-1/2}\left(T_j^{n+(i-1)/N} - T_{j-1}^{n+(i-1)/N}\right)\end{array}\right].
\end{aligned} \tag{7}$$

The results of solving the equation using the coefficients in (7) rather than those in (4), evaluating all derivatives of the form $\partial\chi/\partial T'$ numerically, and using just a single Newton iteration each time step, are shown in Figs. 3 and 4. We see that the solution converges to a mean result (compared to Figs. 1 and 2) and without oscillations. Note that if we specialize to only a single Newton iteration, we can rewrite Eq. (7) as:

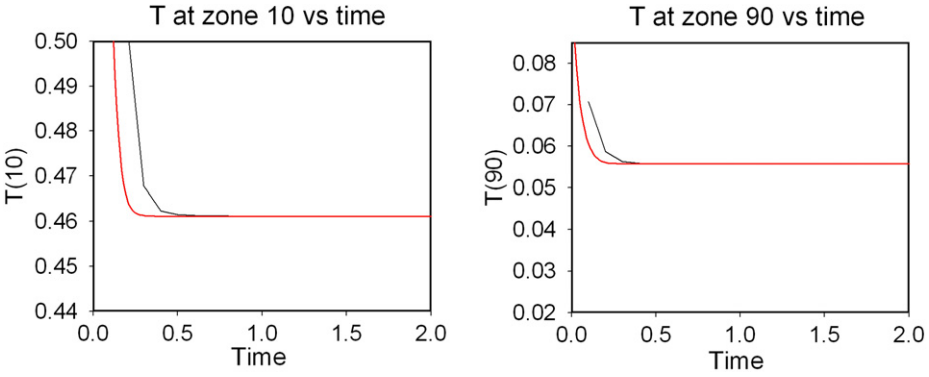

Fig. 3. Temperatures at zone 10 (left) and zone 90 (right) corresponding to Fig. 1 using a single Newton iteration as defined by Eq. (8).

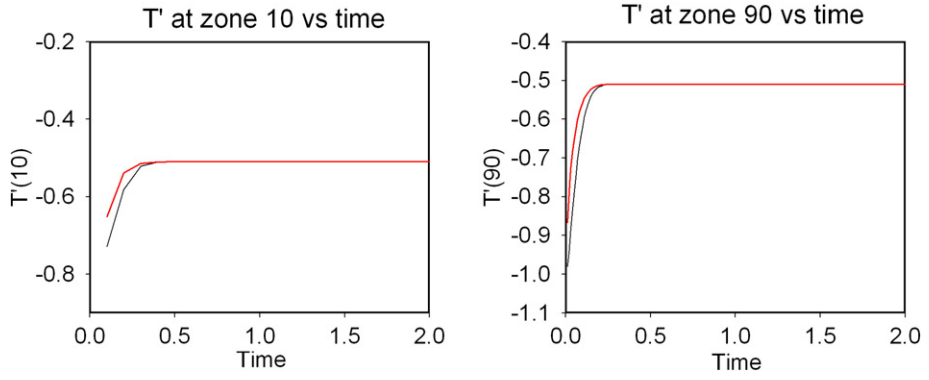

Fig. 4. Temperatures derivatives at zone 10 (left) and zone 90 (right) corresponding to Fig. 2 using a single Newton iteration as defined by Eq. (8).

$$
\begin{aligned}
T_j^{n+1} = & T_j^n + s\theta \left\{ \begin{array}{l} \Phi_{j+1/2}\left[\chi\left(T'^n_{j+1/2}\right) + \frac{\partial\chi}{\partial T'} T'^n_{j+1/2}\right]\left(T^{n+1}_{j+1} - T^{n+1}_j\right) \\ -\Phi_{j-1/2}\left[\chi\left(T'^n_{j-1/2}\right) + \frac{\partial\chi}{\partial T'} T'^n_{j-1/2}\right]\left(T^{n+1}_j - T^{n+1}_{j-1}\right) \end{array} \right\} \\
& + s(1-\theta) \left\{ \begin{array}{l} \Phi_{j+1/2}\left[\chi\left(T'^n_{j+1/2}\right) + \frac{\partial\chi}{\partial T'} T'^n_{j+1/2}\right]\left(T^{n}_{j+1} - T^{n}_j\right) \\ -\Phi_{j-1/2}\left[\chi\left(T'^n_{j-1/2}\right) + \frac{\partial\chi}{\partial T'} T'^n_{j-1/2}\right]\left(T^{n}_j - T^{n}_{j-1}\right) \end{array} \right\} \\
& - s\left[\Phi_{j+1/2}\frac{\partial\chi}{\partial T'} T'^n_{j+1/2}\left(T^n_{j+1} - T^n_j\right) - \Phi_{j-1/2}\frac{\partial\chi}{\partial T'} T'^n_{j-1/2}\left(T^n_j - T^n_{j-1}\right)\right] + \Delta t S. \qquad (8)
\end{aligned}
$$

We note that the finite difference Eq. (8) corresponds to the differential equation:

$$
\frac{\partial T}{\partial t} = \frac{\partial}{\partial \Phi}\left\{\Phi\left[\chi(T') + \frac{\partial\chi}{\partial T'}T'\right]\frac{\partial T}{\partial \Phi}\right\} - \frac{\partial}{\partial \Phi}\left\{\Phi\left[\frac{\partial\chi}{\partial T'}T'\right]\frac{\partial T}{\partial \Phi}\right\} + S, \qquad (9)
$$

where the first term on the right is evaluated θ-centered in time and the second term is evaluated at the old time level. The multi-iteration Newton method, Eq. (7), is equivalent to repeating the timestep but using the most recent values of χ and $\partial\chi/\partial T$ in (9).

As further demonstration of the improved properties of the Newton method (8) over the backward Euler method (3), we show a comparison of the solutions over the transient period $0 < t < 0.4$ with a series of timesteps ranging from $\Delta t = 0.0025$ to $\Delta t = 0.08$. Fig. 5a corresponds to the Newton method (8). The results are seen to converge linearly in time step Δt. Fig. 5b corresponds to the backward Euler method (3) with $\theta = 1$. It appears from this figure that the results are non-convergent as $\Delta t \to 0$. In order to show that both methods are in fact consistent with the original PDE, we have extended the convergence studies to very small values of time step ($\Delta t = 1 \cdot e - 6$) and plot the two results for $T(10)$ at $t = 0.16$ as a function of time step in Fig. 5c, but with a logarithmic scale for Δt. It is seen that the Newton Method converges to the correct solution with a time step about 4 orders of magnitude larger than that required for the Backward Euler method to exhibit convergence.

We have incorporated this method into two existing production tokamak transport codes with only minor modification. Thus, in the existing numerical method in TSC [5] or in PTRANSP [6], the first term can just be treated as a modified thermal conductivity:

$$
\chi(T') \to \chi(T') + \frac{\partial\chi}{\partial T'}T' \qquad (10a)
$$

and the second term can be treated as a modified source term:

$$
S \to S - \frac{\partial}{\partial \Phi}\left\{\Phi\left[\frac{\partial\chi}{\partial T'}T'\right]\frac{\partial T}{\partial \Phi}\right\}. \qquad (10b)
$$

Extending this to two temperatures T and T_e gives:

$$
\begin{aligned}
\frac{\partial T}{\partial t} &= \frac{\partial}{\partial \Phi}\left\{\Phi\left[\chi(T') + \frac{\partial\chi}{\partial T'}T'\right]\frac{\partial T}{\partial \Phi} + \Phi\left[\frac{\partial\chi}{\partial T'_e}T'\right]\frac{\partial T_e}{\partial \Phi}\right\} - \frac{\partial}{\partial \Phi}\left\{\Phi\left[\frac{\partial\chi}{\partial T'}T'\right]\frac{\partial T}{\partial \Phi} + \Phi\left[\frac{\partial\chi}{\partial T'_e T'}\right]\frac{\partial T_e}{\partial \Phi}\right\} + S, \\
\frac{\partial T_e}{\partial t} &= \frac{\partial}{\partial \Phi}\left\{\Phi\left[\chi_e(T') + \frac{\partial\chi_e}{\partial T'_e}T'_e\right]\frac{\partial T_e}{\partial \Phi} + \Phi\left[\frac{\partial\chi_e}{\partial T'}T'_e\right]\frac{\partial T}{\partial \Phi}\right\} - \frac{\partial}{\partial \Phi}\left\{\Phi\left[\frac{\partial\chi_e}{\partial T'_e}T'_e\right]\frac{\partial T_e}{\partial \Phi} + \Phi\left[\frac{\partial\chi}{\partial T'}T'_e\right]\frac{\partial T}{\partial \Phi}\right\} + S.
\end{aligned} \qquad (11)
$$

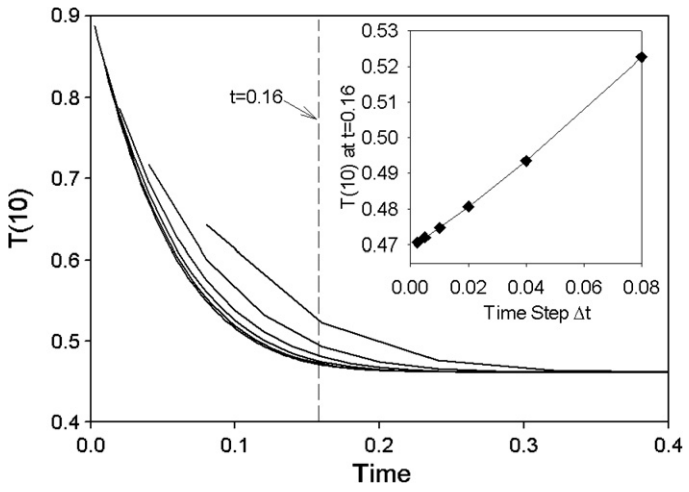

Fig. 5a. Convergence results for Newton method (3) for a sequence of time steps ranging from 0.0025 to 0.080. Inset shows values at time $t = 0.16$.

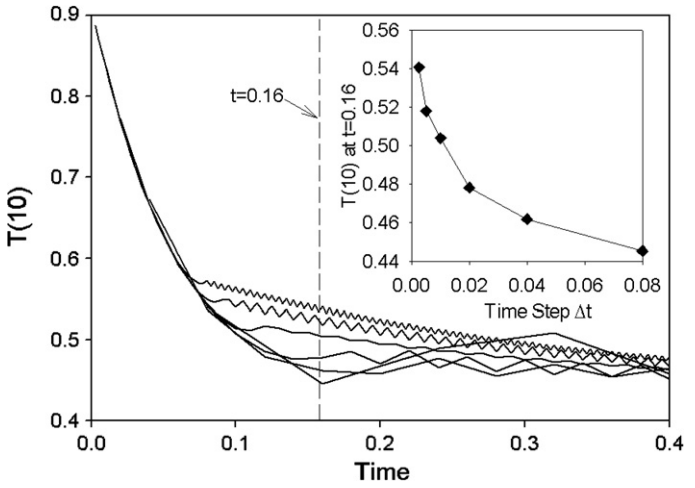

Fig. 5b. Same as for Fig. 5a except using the backward Euler method. Results do not appear to be converging with timestep.

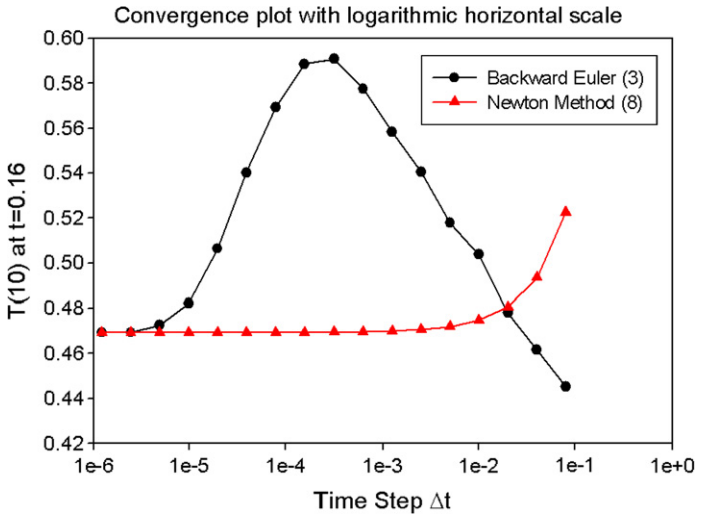

Fig. 5c. Expansion of the inset graphs from Figs. 5a and 5b to very small values of Δt to illustrate that both methods eventually converge to same value.

Here, again, the first term on the right of each equation is evaluated θ-centered in time, and the second term is evaluated at the old time level.

The algorithm presented here is a variation of an unpublished algorithm first developed by one of us for usage in transport codes employing the IFS-PPPL transport model, which is a precursor to the current GLF23 model. In this note we show it to be in fact a Newton iteration and hence it can be iterated each individual time step to improve robustness. Variants of this algorithm have also been briefly mentioned in Refs. [7,8]. Taking a single iteration is a similar concept to that proposed by Beam and Warming [9] for systems of hyperbolic equations, while performing multiple iterations is equivalent to the nonlinearly consistent method [10], both of which are discussed in Ref. [11]. Another approach to iterative algorithms for these types of problems is discussed in Ref. [12]. A significant new feature of the method presented here is that the linearization has been done semi-analytically (but without assuming any particular form for $\chi(T)$). This allows us to keep the implicit difference equations in tri-diagonal form, even after the linearization. One does not need to calculate Jacobians or use Krylov methods such as GMRES as is done in [11]. Since the tri-diagonal solution method is very efficient and already being used by the codes we are targeting, the modification only amounts to a simple re-definition of the coefficients and essentially no increase in running times.

Application to a JET discharge

Here we show an example with the method implemented in the PTRANSP code as part of the finite difference algorithm that is used to advance the electron and ion thermal transport equations. The thermal transport equations are a pair of

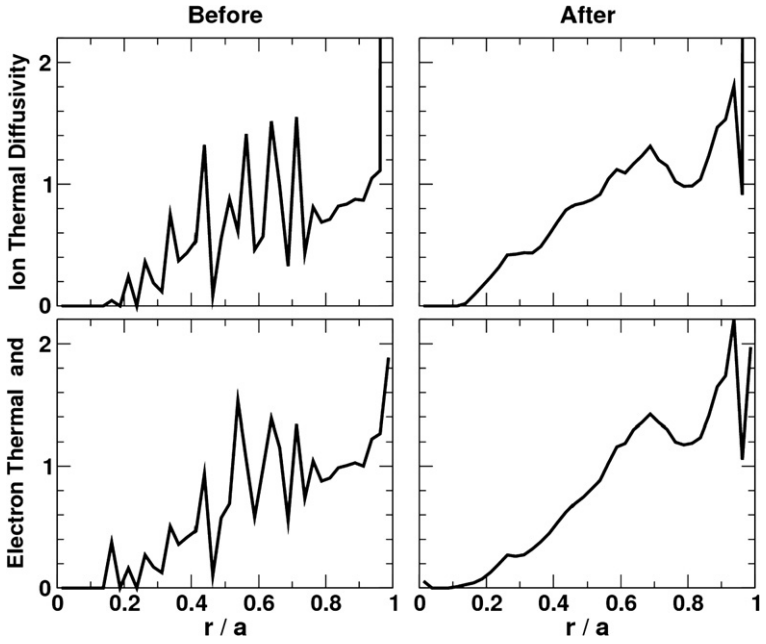

Fig. 6. Electron and ion thermal diffusivity (bottom and top panels, respectively) as a function of normalized minor radius, r/a, from a PTRANSP simulation of a JET discharge before and after Newton's method was implemented (left and right panels, respectively).

diffusive-convective equations, similar to Eq. (11), that are coupled tightly through an equipartition term that is proportional to the difference between the electron and ion temperatures. When the finite difference approximations to the transport equations are advanced in time using an implicit technique, the result is a block tridiagonal system of algebraic equations similar to Eq. (4) that must be solved each time step.

Before the implementation of the form of Newton's method described here, time smoothing was used in an effort to control the numerical artifact associated with the use of stiff transport models. The results of a simulation using time smoothing together with the GLF23 transport model are shown in the left two panels of Fig. 6, where the electron and ion thermal diffusivities are plotted as a function of normalized minor radius (electron thermal diffusivity in the bottom panel and ion thermal diffusivity in the top panel). If time smoothing (or Newton's method) were not used, the numerical artifact (ragged behavior shown in the left panels of Fig. 6) would be so severe that the simulation could not be run.

Corresponding simulation results are shown in the right panels of Fig. 6 after the implementation of Newton's method [similar to Eq. (7)] with time smoothing turned off. In this simulation of a JET tokamak discharge using the GLF23 transport model, three Newton's method iterations are used to advance the finite difference equations each time step and the implicitness parameter θ is taken to be unity. (The use of three iterations is a compromise between a single iteration, which gives almost identical results, and a full nonlinear convergent method, which has not been implemented. Simulation results indicate that $\theta = 1$ yields smoother solutions for a single Newton iteration with large timesteps than does $\theta = 0.5$). The small remaining lack of smoothness in the diffusivity profiles can be attributed to the random Monte Carlo noise in the source terms [S in Eq. (11)] and the abrupt transition to a steep gradient boundary layer that is imposed beyond $r/a > 0.95$ in these simulations.

Several problems were encountered in the implementation of Newton's method in the TSC and PTRANSP codes when used with the GLF23 transport model. There are some conditions, for example, that result in a negative derivative of the thermal diffusivity with respect to the temperature gradient, at least for one of the channels of transport. The negative gradient can be so large that the combination $\chi + (\partial\chi/\partial T)T$ can be negative (such as could happen at a transport barrier bifurcation), which results in a severe numerical instability. In order to avoid this problem, the magnitude of negative values of $\partial\chi/\partial T$ had to be limited in order to ensure that the combination $\chi + (\partial\chi/\partial T)T$ is always positive.

Acknowledgments

The authors acknowledge helpful conversations with Drs. X.C. Cai, D. Keyes, H. St. John and D. McCune. We thank Prof. A.H. Kritz for his encouragement in publishing this technique. This work was supported by US DoE contract DE-AC02-76CH0307.

References

[1] S. Hirshman, S. Jardin, Two-dimensional transport of tokamak plasmas, Phys. Fluids 22 (1979) 731.

[2] R.E. Waltz, G.M. Staebler, W. Dorland, G.W. Hammett, M. Kotschenreuther, Phys. Plasmas 4 (1997) 2482.
[3] J.E. Kinsey, G. Staebler, R.E. Waltz, Fusion Sci. Technol. 44 (2003) 763.
[4] R.D. Richtmyer, K.W. Morton, Difference Methods for Initial Value Problems, second ed., Interscience, New York, 1967. 405pp.
[5] S.C. Jardin, N. Pomphrey, J. DeLucia, Dynamic modeling of transport and positional control of tokamaks, J. Comput. Phys. 66 (1986) 481.
[6] D.M. McCune et al., PTRANSP documentation, <http://w3.pppl.gov/transp/>.
[7] J.E. Kinsey, G.M. Staebler, R.E. Waltz, Phys. Plasmas 9 (2002) 1676–1691.
[8] J.E. Kinsey, G.M. Staebler, R.E. Waltz, Phys. Plasmas 12 (2005) 052503.
[9] R.M. Beam, R.F. Warming, An implicit finite-difference algorithm for hyperbolic systems in conservation law form, J. Comput. Phys. 22 (1976) 87–110.
[10] D. Knoll, W. Rider, G. Olson, An efficient nonlinear solution method for non-equilibrium radiation diffusion, J. Quant. Spectrosc. Radiat. Transfer 63 (1999) 15–29.
[11] R.B. Lowrie, A comparison of implicit time integration methods for nonlinear relaxation and diffusion, J. Comput. Phys. 196 (2004) 566–590.
[12] A.I. Shestakov, R.H. Cohen, J.A. Crotinger, et al, J. Comput. Phys. 186 (2003) 360.